Blend Films of Waterborne Polyurethane-Carboxymethylated Guar Gum Crosslinked by Ca^{2+}

AIBIN HUANG* and WANWAN LE

Hangzhou Dianzi University, Hangzhou 310018, P.R. China

*Corresponding author: Tel: +86 571 86878591; E-mail: huangaibin@hdu.edu.cn

Films from waterborne polyurethane (WPU) and carboxymethylated guar gum (CMGG) with different contents (20-80 wt %) were prepared through solution casting method and then were crosslinked with calcium chloride. The effect of CMGG content on the miscibility, morphology and physical properties of the blend films is investigated by Fourier transform infrared spectroscopy, scanning electron microscopy, density measurements, differential scanning calorimetry, dynamic mechanical thermal analysis, thermogravimetric analysis, water sensitivity measurements, solvent-swelling and tensile tests. The results reveal that the uncrosslinking films exhibit good miscibility when CMGG content is lower than 60 wt %, whereas typical "sea-island" structure occurs when the CMGG content further increases. After crosslinking with calcium ion, the blend films form a relatively dense architecture, which leads to better miscibility, higher storage modulus and thermal stability. The crosslinking films also exhibit better tensile strength (11.6-56.5 MPa) and solvent-resistance than that of the uncrosslinking films over the entire composition range. A model describing the configuration of Ca^{2+}-chelating structure was proposed to illustrate the different structures of the two series of the blend films.

Keywords: Blend, Waterborne polyurethane, Carboxymethylated guar gum, Ca^{2+}.

INTRODUCTION

Continuous awareness of ecological problem has led to a paradigm shift on the use of biodegradable materials, especially from renewable agriculture feedstock and marine food processing industry wastes[1]. Consequently, natural polymers and their derivatives have attracted considerable attention[2]. Among the several candidates including natural polymers and their derivatives, guar gum (GG), a high-molecular weight water-soluble non-ionic natural polysaccharide isolated from the seed endosperm of the guar plant, is one of the promising materials for biodegradable plastics because it is a versatile biopolymer with immense potential and low price for use in the non-food industries[3]. It is a member of the class of galactomannans, which consist of a (1-4)-linked β-D-mannopyranosyl backbone partially substituted at O-6 with α-D-galactopyranosyl side groups[4]. Because of these associations, guar gum possesses remarkable rheological properties[5] and is widely used in food[6], personal care[7] and oil recovery. In recent years, modified guar gum has been found numerous applications in cartridge explosives, mining, froth flotation, oil recovery, textile printing and water-based paints[8]. Among many chemically modified methods, chemical crosslinking is a convenient and feasible method to modify the structure of natural polymers and thus makes them attractive biomaterials for further applications. In previous papers, through crosslinking with glutaraldehyde, phosphate, urea-formaldehyde and borax, modified guar gum was applied in various fields, such as controlled drug release[9], colon-specific drug delivery[10], liquid pesticide[11], water retention[12], *etc*. However, the high water sensitivity and bad form-films ability of guar gum and its derivatives limit their applications as useful film materials. At present there exists several different ways to overcome these problems, one of them is mixtures of synthetic polymers with natural polymers (preparation of polymer mixtures) which have good biodegradable properties; another option is the synthesis of polymers with use of products from natural sources[13].

Polyurethane (PU), an unique polymeric material with a wide range of physical and chemical properties, has been extensively tailored to meet the highly diversified demands of modern technologies[14]. Driven by continuous reduction in costs and the control of volatile organic compound emissions, the development of waterborne polyurethane has been increasing[15]. It is noted that waterborne polyurethane, as a nontoxic, non-flammable and environmentally friendly material, has been abundantly used as an environmental coating and an adhesive, automatic finishing, industrial finishing and corrosion-protection coating[16]. However, because of its poor tensile strength and bad organic solvent-resistance, the use of waterborne polyurethane (WPU) as a material is limited to certain extent. So, it is an

effective path to overcome the disadvantage through combined use of natural polymers. Many researchers have reported that the composites materials prepared from WPU with natural polymers or their derivatives, such as starch[17] casein[18], soy protein[19], carboxymethyl konjac glucomannan[20], carboxymethyl chitin[21] have been studied. These researches exhibited that natural polymers or their derivatives play an important role in improving thermal stability, tensile strength and solvent-resistance of the composites materials.

Polymer blending is an important method for modification or improvement of the physical properties of polymeric materials. Blends of polymers may result in cost reduction and better processing, thus enhancing the properties to be maximized[22]. On several occasions the initial dispersion of the blend component is further promoted by crosslinking, creation of interpenetrating networks, mechanical interlocking comments and use of 'compatibizing agents' in order to ensure that no demixing will occur at a later stage[23].

The effects of Ca^{2+} crosslinking on structure and properties of the blend materials from waterborne polyurethane and natural polymers have been less reported. A basic understanding of the behavior for Ca^{2+} crosslinking blend films is essential for a successful research and development of the new materials. So, in this study, we attempt to introduce Ca^{2+} into the blend films by employing aqueous ethanolic solution of calcium chloride. It can be expected that the post-treatment with $CaCl_2$ will allow the production of crosslinking in both components. The structure and morphologies of the uncrosslinked and crosslinked films were characterized by ATR-FTIR and SEM. The miscibility and properties of the blend films were evaluated with DSC, DMTA and density measurements, respectively. Furthermore, the thermal properties, mechanical properties, contact angle, moisture uptake and solvent-resistance of the two series of blend films were also evaluated by TGA, tensile tests, contact angle measurements, moisture uptake measurements and solvent-swelling tests, respectively.

EXPERIMENTAL

All of chemical reagents were obtained from commercial sources in China. Guar gum (GG) was kindly supplied by Wuhan Tianyuan Biology Co., China. The method of preparation and purification was followed as document[24]. Commercial 2,4-toluene disocyanate (TDI; Shanghai Chemical Co., China) was vacuum-dried at 80 ℃ for 2 h and was used as hard segments. Polyethylene-propylene adipate glycol (PEPA; Mn = 1980; Jinlin Chemical Co., Nanjin, China) was vacuum-dried at 110 ℃ for 2 h and was used as soft segments. 2,2-*Bis*(hydroxyl methyl) propionic acid (DMPA; Chengdu Polyurethane Co., China) was also dried under vacuum at 110 ℃ for 5 h and used as chain extender and anionic center. Triethylamine (TEA; Shanghai Chemical Co., China) and butanone as a neutralized reagent and a solvent, respectively, were treated by 3 Å molecular sieves for more than a week to dehydrate them before use. Chloroacetic acid, sodium hydroxide and methanol were analytical grade. The other reagents were used without further purification.

Synthesis of waterborne polyurethane: Anionic waterborne polyurethane (WPU) was synthesized according to the acetone process reported earlier[1]. The molar ratio of NCO/OH in this case was 1.75. A 500-mL four-necked flask was fitted with a thermometer, a stirrer and an inlet and outlet of dry nitrogen. The dry PEPA (47.3 g) and DMPA (3.17 g) were added into the flask and stirred at 120 ℃ for 15 min to dissolve DMPA easily, then cooled to 85 ℃; TDI (14.4 g) was added in one portion and stirring was continued at 85 ℃ for 2-3 h under dry nitrogen until the content of NCO groups reached a given value, as determined by dibutylamine back titration. Subsequently, the butanone was poured into the flask to reduce the viscosity of prepolymer and then cooled to 60 ℃. After neutralized with TEA for 0.5 h, the product was dispersed with distilled water to emulsify. The solid content was controlled to 20 wt % under vigorous stirring for 0.5 h and its viscosity measured by using a rotation viscosity meter (NDJ-4, Shanghai Balance Factory) was 6.8 MPas.

Preparation of carboxymethylated guargum: CMGG was prepared using a slightly improved method over the reported by Kobayashi *et al.*[22] and Lin *et al.*[25]. In a 500 mL three-necked round-bottom flask equipped with a reflux condenser and N_2 supply, 10 g of guar gum was suspended in 50 mL of 50 wt % aqueous methanol. After 0.5 h, 40 g of 50 wt % aqueous solution of sodium hydroxide was added gradually while stirring at room temperature. After 2 h, 30 g of chloroacetic acid, dissolved in 50 mL of 50 wt % aqueous methanol, was added gradually. Mechanical stirring was continued for 24 h at 50 ℃ and then it was allowed to cool to room temperature. At this point, the solution was neutralized with acetic acid. The product was washed with 70, 80 and 100 wt % methanol to remove impurities, successively and filtered off. The residue was air-dried and dried at 50 ℃ *in vacuo*. Its degree of substitute was 0.78 according to the titration method. FTIR spectrum of CMGG was shown in Fig. 1, it was obvious that the absorption bands centered at 1619 cm^{-1}, were ascribed to asymmetric stretching vibration of the free carboxylate ion and the peaks at 1420 and 1370 cm^{-1} were concerned with the symmetric stretching vibration of the free carboxylate ion in CMGG sample[26]. These changes confirmed that CMGG was synthesized.

Preparation of the blend films: 2.0 g of CMGG was dissolved in 100 g deionized water to obtain 2 wt % CMGG solution. Subsequently, the WPU was mixed with varying amounts of CMGG solution at room temperature with continuous stirring for 2 h. Last, the mixture was degassed and then casted on a glass plate mold, followed by drying at room temperature in an oven for several days to obtain a transparent film. By changing the weight per cent of CMGG in the blend films such as 20, 40, 60 and 80 wt %, a series of blend films were prepared, coded as UG-20, UG-40, UG-60 and UG-80, respectively. The films from pure CMGG and WPU were coded as CMGG and WPU, respectively. After being dried, the films were immersed in 5 wt % calcium chloride 70 wt % aqueous ethanol solution for 0.5 h. After coagulation, the prepared films were washed with deionized water to remove the unreacted calcium chloride. The films undergoing post-treatment were coded as CUG-20, CUG-40, CUG-60 and CUG-80, respectively. The crosslinked films from pure CMGG and WPU were coded as CCMGG and CWPU, respectively. The compositions
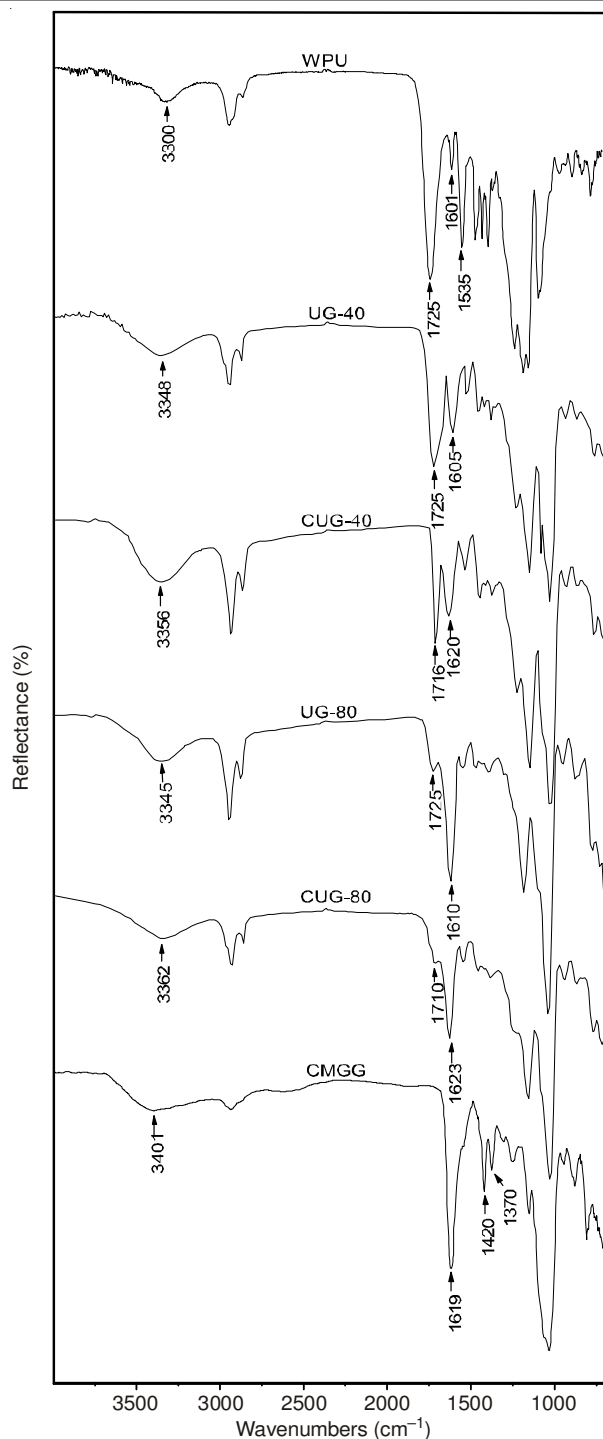
Fig. 1. ATR-FTIR spectra of the UG and CUG films

TABLE-1
COMPOSITION OF THE UG AND CUG FILMS

Samples	W_{CMGG} (wt %)	W_{Ca} (wt %)	ρ (g/cm^3)
WPU	0	–	1.13
UG-20	20	–	1.21
UG-40	40	–	1.32
UG-60	60	–	1.42
UG-80	80	–	1.43
CMGG	100	–	1.46
CWPU	0	0.092	1.14
CUG-20	20	0.097	1.27
CUG-40	40	0.115	1.41
CUG-60	60	0.132	1.44
CUG-80	80	0.154	1.48
CCMGG	100	0.167	1.54

temperature on a Nicolet ATR-FTIR spectrometer (Avatar 360, United States) fitted with a germanium crystal, with a fixed 45° angle of incidence. The samples with thickness of 100 mm were taken at random from sheets and placed flat on the crystal surface. The data were collected over 32 scans with a resolution of 4 cm^{-1}.

SEM micrographs were taken on a Hitachi S-570 microscope (Japan). The blend films were frozen in liquid nitrogen and snapped immediately and the surface and cross section of the films were sputtered with gold, observed and photographed. For the observation of the structure of the uncrosslinked films, the UG films, enclosed in a nylon mesh, were immersed in acetone and this was accompanied by mild stirring for 24 h at room temperature; thus, WPU was dissolved in acetone and removed from the UG films during extraction, leaving voids.

The density (ρ) of the blend films was measured at 25 °C by determining the weight of a volume-calibrated psychomotor filled with a mixture of chloroform and ethanol, in which the samples achieved floatation level. The density of the liquid mixture equals the density of the samples. Three parallel measurements were carried out for every sample.

DSC thermograms over the temperature range -130 to 100 °C were recorded using DSC-204 apparatus (Netzsch Co., Germany) under a nitrogen atmosphere. The experiments were carried out at a heating rate of 10 °C/min. DMTA was carried out with a dynamic mechanical thermal analyzer (DMTA-V, Rheometric Scientific Co., USA) at 1 Hz and a heating rate of 5 °C/min in the temperature range from -80 to 100 °C. Specimens with typical size of 10 mm ×10 mm (length × width) were used. TGA thermograms of the specimens were recorded on a thermoanalyzer (DT-40; Shimadzu) under nitrogen atmosphere with a flow capacity of 50 mL/min from 20 to 600 °C, at a heating rate of 10 °C/min. The starting decomposition temperature and weight loss values of the samples were evaluated by using the intersection point of tangents of TGA curves.

The contact angle measurements were performed with a Kruss G23 (Germany) apparatus. A water droplet was put on the surface of a sample and the droplet shape was recorded. A CCD video camera and imagine analysis software were used to determine the contact angle evolution.

The moisture uptake measurements of the blend films were performed as follows: the dried films of 20 mm × 10 mm, kept at 0 % RH (P$_2$O$_5$) for 1 week, were weighed and then conditioned in a chamber of 75 % RH at 25 °C. The sample was removed at desired intervals and weighed until the

of the uncrosslinked and crosslinked films are listed in the Table-1. The thickness of the blend films was controlled to be 0.1 mm. All the films were vacuum-dried at room temperature for 3 days and kept in a desiccator with P$_2$O$_5$ as a desiccant for more than 1 week before the characterization.

Characterization: Calcium content in the crosslinked films was determined by ICP-AES (United States). The crosslinked films were burned in a muffle furnace at 650 °C and then dissolved in nitric acid, followed by diluting to a certain concentration with distilled water.

Attenuated total reflection Fourier transform infrared (ATR-FTIR) spectroscopy of the films was performed at room

equilibrium state was reached. The moisture uptake of the blend films was calculated as follows:

$$\text{Moisture uptake (wt \%)} = \left[\frac{(w_t - w_0)}{w_0}\right] \times 100\%$$

where w_0 and w_t are the initial weight and weight in 75 % RH of the sample, respectively.

Solvent-swelling tests of the blend films were performed with different organic solvents including acetone, methanol, N,N-dimethylformamide and toluene at room temperature for 12 h. The dry films were weighed and then immersed into the solvents to prepare swelling films for 12 h. The resulting films were taken out and the excess solvent on the films was wiped off to weigh. The degree of swelling was calculated by the following equation:

$$\text{Degree of swelling (wt \%)} = \left[\frac{(w_s - w_0)}{w_0}\right] \times 100\%$$

where w_s represent the weight of the swollen film and w_0 is the weight of the dry film.

The tensile tests of the films were measured on a universal testing machine (CMT6502, Shenzhen SANS Test Machine Co. Ltd., China) with a tensile rate of 5 mm/min[-1] according to ISO6239-1986 (E') to obtain tensile strength (σ_b) and breaking elongation (ε_b). The mean values of σ_b and ε_b were obtained from three replications, respectively.

RESULTS AND DISCUSSION

Structure and morphology of the blended films: It is well known that IR spectrometer is a powerful instrument for the investigation of the hydrogen bonding based on the frequency shift of the groups[27]. FTIR spectra of the UG-40, CUG-40, UG-80, CUG-80, WPU and CMGG films are shown in Fig. 1. The WPU displayed characteristic peaks at 1725 cm^{-1}, which was attributed to the stretching of free urethane carbonyl groups, while the band centered at 3300 and 1601 cm^{-1} were assigned to hydrogen-bonded -NH in urethane group and hydrogen-bonded carboxylic carbonyl groups in WPU films, respectively[28]. With CMGG content increased, intensity of peak at 1725 cm^{-1} decreased, while that of peak at 1601 cm^{-1} increased in the UG films. Moreover, compared with pure WPU, the -NH stretching vibration exhibited strong absorption peaks and shifted to a higher wavenumber from 3300 cm^{-1} to about 3340 cm^{-1} with an increase on CMGG content. This indicated an enhancement of the free -NH group fraction in the UG films[29]. An obvious shoulder peak appeared at 3290 cm^{-1}, corresponding to the NH-O hydrogen bonding between the amide groups of WPU networks and the carboxylic groups of CMGG. This implied that the original inter-and intra-molecular hydrogen bonds involved in WPU films were destroyed due to the strong interaction between WPU and CMGG.

The delineation of the ATR-FTIR spectrum for the CUG films was slightly different from that of the UG films in the Fig. 1. The band of -NH stretching vibration for CUG-40 and CUG-80 films shifted to higher wavenumber than that of UG-40 and UG-80, which indicated that the intensity of free -NH in urethane group increased and hydrogen-bonded -NH in urethane group of WPU decreased. This can be explained that

the Ca^{2+}-chelating formation between calcium ion and carboxylic groups in the CUG films restricted the formation of urethane -NH, which lead to an increase of free -NH. Meanwhile in the spectra of CUG films, compared with the UG films, the extent of urethane carbonyl groups became smaller and shifted to relatively low wavenumber. Simultaneously, the band of carboxyl groups centered at about 1620 cm^{-1} in CUG-40 and CUG-80, compared with the band of carboxyl groups in the UG-40 and UG-80 films, shifted to a higher wavenumber. These results showed that the crosslinking reaction was conducted by the carboxylate group and calcium ion[30].

Fig. 2 shows SEM micrographs of the free surfaces of the UG and CUG films, respectively. A smooth and homogeneous morphology for UG-40 was observed, which suggested that a strong interfacial interaction existed between WPU and CMGG. When CMGG content reached 60 wt %, it is possible to observe a nucleating structure resulting from aggregation of smaller nuclei for the UG-60 film. But when the CMGG content reached 80 wt %, the morphology of the blend film surface appeared a typical "sea-island" structure, namely, an island of WPU particles dispersed in the sea of the CMGG matrix[31]. In the CUG films, we can observe the more compact structure in the S-CUG-40 than that of S-UG-40. When the CMGG content reached 60 wt %, the nucleating structure was disappeared in the S-CUG-60 films. This was explained that Ca^{2+} crosslinking improved the structure inside the blend films by the formation of a relatively dense architecture structure, leading to better component compatibility[32,33]. In the S-CUG-80, compared with the S-UG-80, it is observed that the shape of the "island" became small and the "sea-island" structure became vague, which exhibited that Ca^{2+} crosslinking structure might reinforce the interfacial adhesion in the blend films.
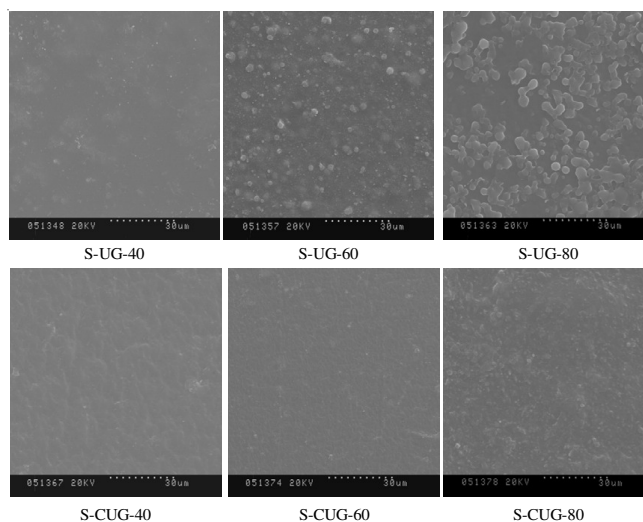

Fig. 2. SEM images of surface sections of the UG and CUG films ("S" is expressed to the abbreviation of "surface")

In addition, SEM micrographs of the cross sections of the UG and CUG films are shown in Fig. 3. In order to observe clearly the inner structure of the UG films, the cross sections of the UG films extracted with acetone are also shown in Fig. 3. A smooth and fluctuant fracture cross sections appeared in the C-UG-40, suggesting a good miscibility between WPU and CMGG. When the CMGG content reached 60 wt %, a
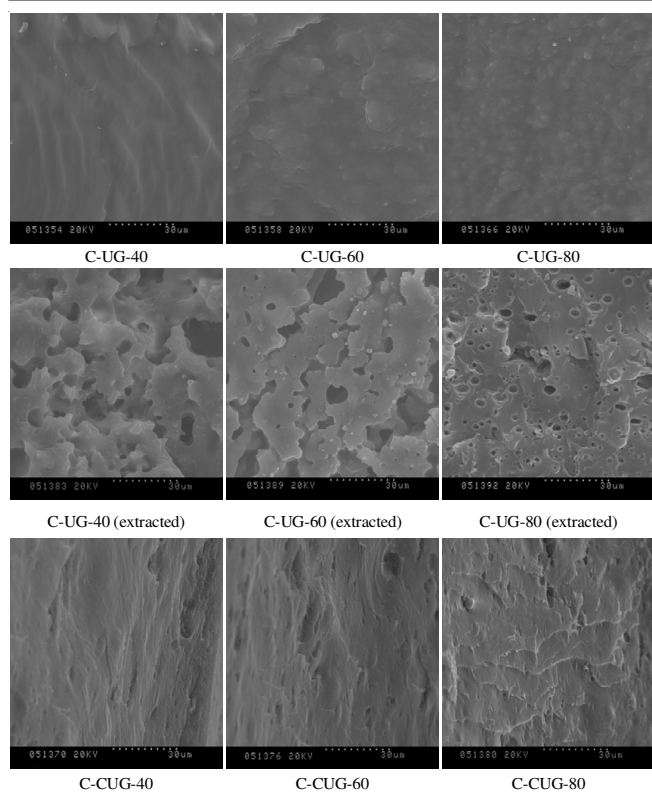
Fig. 3.   SEM images of cross sections of the UG and CUG films ("C"is expressed to the abbreviation of"cross" and "extracted" was expressed that the UG films were extracted with acetone)

rough structure in the C-UG-60 films was observed. Nevertheless, there was plenty of protuberance in the cross sections of the C-UG-80 film, which was explained that a small amount of WPU particles were dispersed in the continuous phase of CMGG to produce strong adhesion force, resulting in formation of the "sea-island" structure. The phenomena were proved by the cross sections of the UG films extracted with the acetone. Clearly, the extraction made the cross sections porous and the extracted degree decreased with an increase of CMGG content. When CMGG content in the UG films were relatively low, CMGG molecules as a dispersed phase are proportionally separated into WPU particles matrix. When CMGG content continued to increase, WPU particles were dispersed in the continuous phase of CMGG matrix, which can be seen in the C-UG-80 (extracted) sample. In fact, the presence of WPU particles in the CMGG matrix may bring about a great increase in contact area between the two polymeric phases, therefore, favoring mixing and interaction at the boundary, with predictable improved performance of the blend materials[34]. Moreover, the morphology of cross section of CUG films is relatively homogenous and dense, compared with that of UG film, indicating a relatively dense architecture in inner surface. This implies that the crosslinking structure by Ca^{2+} was helpful to improve the structure inside the blended films and strengthen the compatibility between WPU and CMGG.

Miscibility between WPU and CMGG in blended films: In a polymer blend, where there is no adhesion between the polymer interface and no molecular mixing at the phase boundary, the densities of the blend would be expected to follow the additivity rule of mixtures[35]. The densities measured from the volume density of the components as a function of

CMGG content are shown in Fig. 4. In the UG films, all experimental values of density are obviously higher than that of calculated, further indicating a strong adhesion existence between WPU and CMGG molecules. This implies that WPU particles penetrated into CMGG matrix to bind together, led to a reduction of the free volume of the blend films. In addition, the CUG films possessed higher densities than that of the UG films, revealing that the films prepared with Ca^{2+} crosslinking have more dense structure than that of the uncrosslinked films.
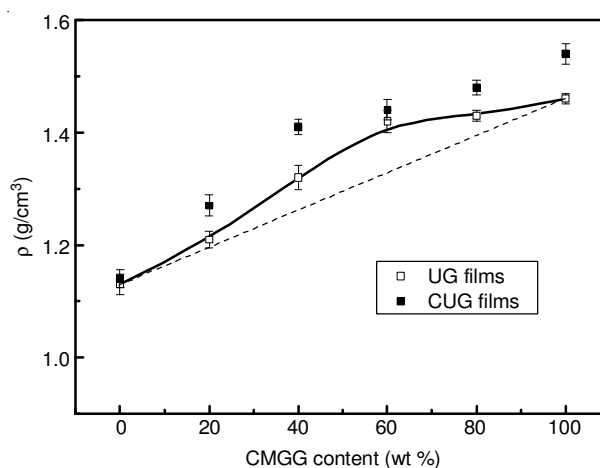

Fig. 4.   Dependence of the densities on CMGG content for the UG and CUG films ("…", the dashed line was expressed to the theoretical densities of the UG films)

DSC curves of the UG and CUG films are shown in Fig. 5 and the corresponding data are given in Table-2. The changes of T_g in polyurethane system are usually attributed to the microphase mixing between soft-segments and hard-segments and the restriction on rotation of the soft-segment linked to hard segment[36]. In the two blend films, T_g of the WPU was shifted to higher temperature with an increase of CMGG content, which was explained that the incorporation of stiff CMGG component resulted in a decrease in the flexibility and mobility of the WPU soft segments. When Ca^{2+} was introduced into the system in the CUG blend, the formation of Ca^{2+}-chelating structure between the two components had great influence on the aggregation of soft segment. Hence, T_g of the WPU in the crosslinked blend films was higher than that of the uncrosslinked blend films.

TABLE-2
GLASS TRANSITION TEMPERATURE AND α
TRANSITION OF THE UG AND CUG FILMS

Samples	DMTA		DSC	
	T_α	tan δ	T_g	ΔC_p ($\times 10^2$ J g^{-1} K^{-1})
WPU	-29.3	0.54	-46.5	0.52
UG-20	-9.9	0.30	-44.8	0.43
UG-40	-7.8	0.19	-37.2	0.34
UG-60	1.3	0.09	-27.3	0.16
UG-80	2.7	0.06	-26.4	0.06
CWPU	-21.2	0.42	-38.3	0.48
CUG-20	-6.5	0.21	-27.9	0.31
CUG-40	-0.7	0.15	-23.7	0.25
CUG-60	1.1	0.07	-21.1	0.09
CUG-80	5.8	0.05	-13.2	0.04

Fig. 5. DSC thermograms of the UG and CUG films

Fig. 6. Storage modulus (E') as a function of temperature for the UG and CUG films

Fig. 7. Tan δ as a function of temperature for the UG and CUG films
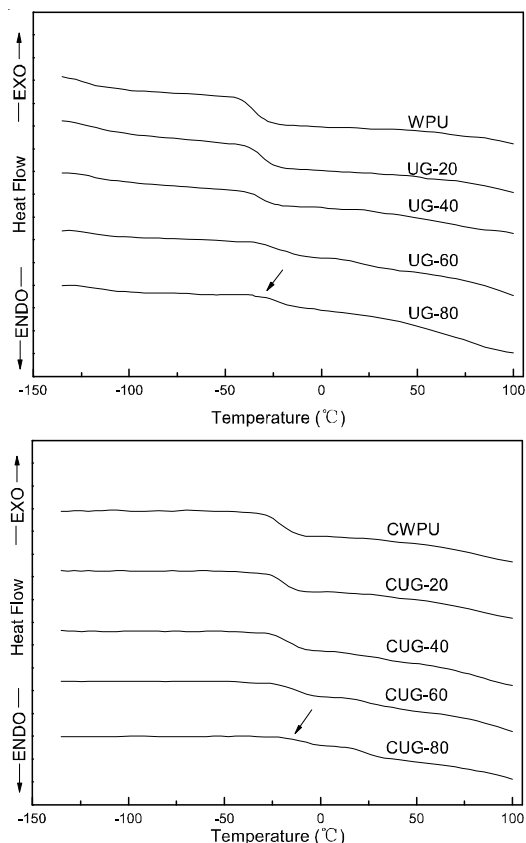
Dynamic mechanical thermal analysis is a valuable technique to investigate the mechanical behavior of materials subjected to cyclic stress and to obtain information about the relaxation mechanisms that may be correlated with the dynamics and the microstructure of the material[37]. The storage modulus (E') of the UG and CUG films as functions of the temperature are plotted in Fig. 6. The storage modulus of the UG films with CMGG content lower than 20 wt % showed a drop in stiffness, accompanying the glass transition (T$_g$) of the WPU soft segments. When the CMGG content was higher than 20 wt %, the UG films exhibited higher E' values and this indicated that CMGG played a role in toughness reinforcement of the blend films. In the CUG films, there was a similar phenomenon like that of the UG films. With CMGG content increased, the toughness of the blend films was strengthened. However, E' values was higher than that of the UG films in the same CMGG content, which was explained that the Ca^{2+} crosslinking between the two polymers formed relatively dense architecture and enhanced the stiffness of the composite materials.

Usually, DMTA can be used to reflect the mobility of chain segment and to obtain the temperature of α-relaxation (T$_α$). tan δ as a function of temperature for the UG and CUG films was shown in Fig. 7 and the peak positions are summarized in Table-2. T$_α$ was about 10 ℃ higher than T$_g$ from DSC. A different mechanism between DSC and DMTA yielding a large difference in the T$_g$ values is practically related to the viscoelastic behavior of the WPU phase and this effect is translated into a large difference in the relaxation times of polymer molecules, particularly in the temperature range near T$_α$[38]. In the
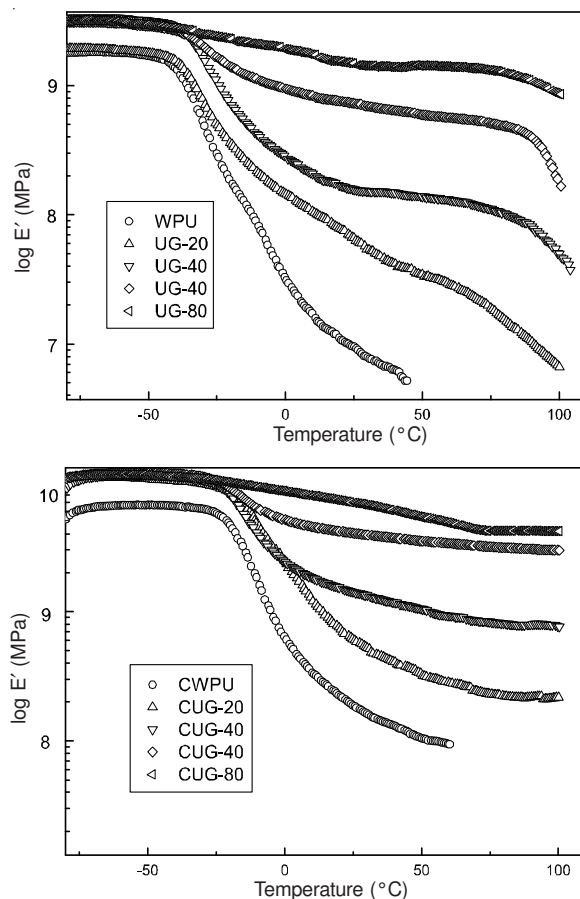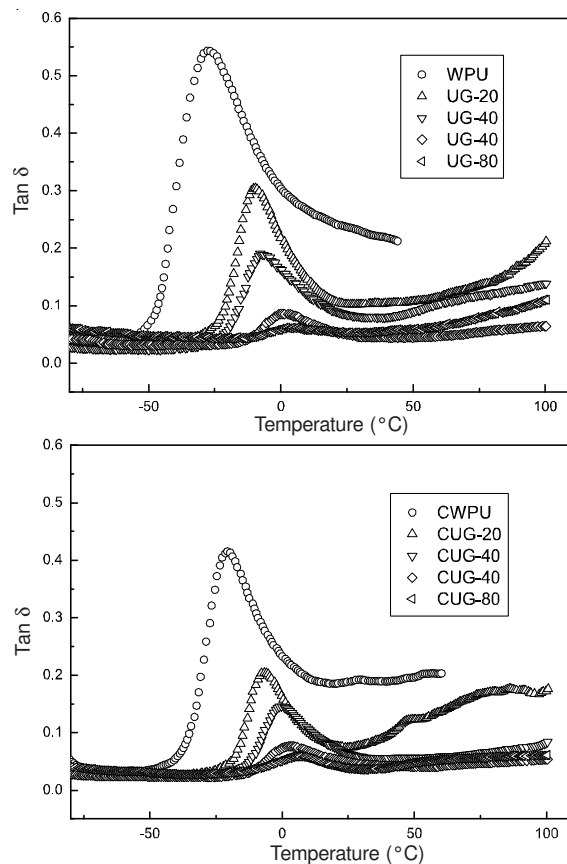
UG films, T_α shifted from -29.3 to 2.7 ℃ with an increase in CMGG content and this is in good agreement with the DSC results. The position and height of the damping peak in the DMTA curves, which are related to the structure, composition and crystallization behavior, may reflect the molecular motion and interaction sensitively. From a plot of tan δ *versus* temperature, the height of the damping peaks of WPU in the films decreased and T_α value obviously shifted to higher temperature. Especially, the damping peaks of WPU almost disappeared in the UG-80 sample. The higher T_α value and decreasing height is associated with lower segmental mobility of WPU soft segment, which was explained that the mobility of soft segment assigned to WPU was restricted because of the hardness of the main chain for CMGG. In the CUG films, the height of the damping peaks of WPU was lower than that of the UG films. Furthermore, the T_α shifts from -21.2 to 5.8 ℃ with an increase in CMGG content, was moved to higher temperature than that of the UG films. This was explained that Ca²⁺ crosslinking structure inhibited the large scale molecular motion of WPU soft segment.

Thermal properties of the blend films: The thermal degradation patterns of the films are shown in Fig. 8. The small weight loss at 30-150 ℃ was assigned to the release of moisture and TEA from the samples. The weight loss at 400-600 ℃ was believed to be caused by oxidation and degradation[39]. The pure WPU film exhibited one weight loss step in the course of thermal degradation and the initial thermal decomposition occurred on 357 ℃ and then, decomposed to give greatest weight loss in 380 ℃, which may be caused mainly by the breaking of urethane bonds[40]. The thermo-gravimetric trace of CMGG revealed that decomposition of CMGG was a single step degradation process, which decomposition started at 247 ℃ and proceeded at a faster rate up to 290 ℃. A small weight loss at 30-250 ℃ was attributed to the release of moisture. From 250 to 290 ℃, the weight loss was resulted from the loss of hydroxyl group of CMGG as water molecules and disintegration of macromolecule chains of CMGG[41]. In the blend films, there were apparent two weight loss step in the course of thermal degradation: the first-step degradation, between nearly 250-300 ℃, corresponded to the CMGG decomposition in blend films and then the second step degradation, between 350-400 ℃, ascribed to WPU degradation. Data related to the temperature corresponding to 10 wt % (T_{10}) and 50 wt % (T_{50}) weight loss of the initial weight, as well as the temperature of initial decomposition (T_i), temperature of final decomposition (T_f) and residues at 600 ℃ are summarized in Table-3. The UG films exhibited much higher thermal stability than that of WPU film, implying that an enhancement of thermal stability caused by strengthening of CMGG as well as interaction between WPU and CMGG. Moreover, there are not perceptible weight loss step in TGA curves of the CUG films, showing the close relation and mutual influence between degradation process of WPU and CMGG. Compared with the UG films, T_{10}, T_{50}, T_i and T_f of the CUG films were improved greatly. The residues in 600 ℃ also were higher than that of the UG films. These showed that relatively dense architecture further improved the thermal stability of the crosslinked films through the formation of Ca²⁺crosslinking inside the blended films.
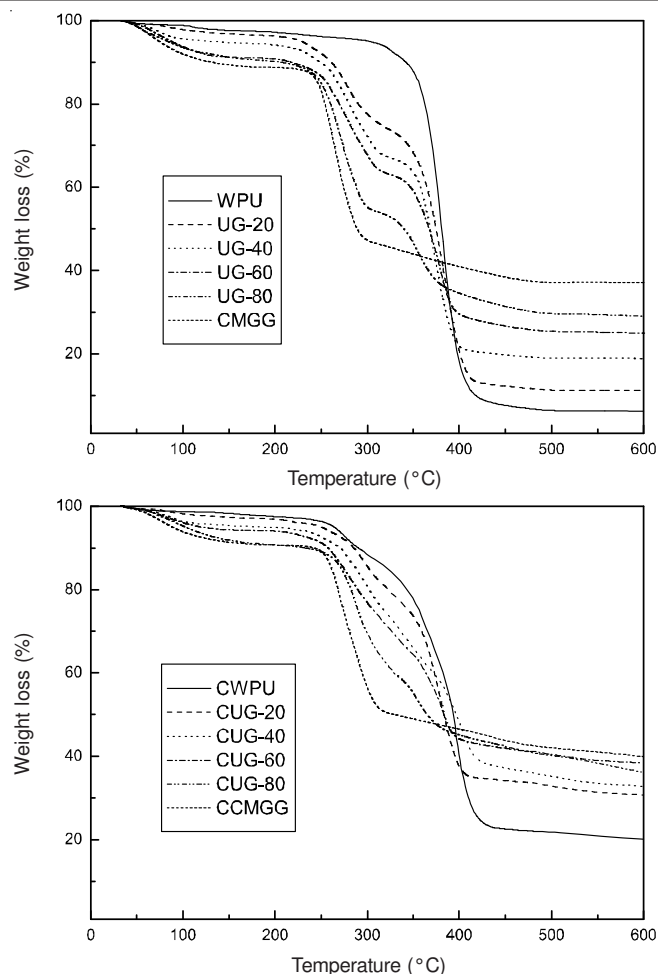

Fig. 8. TGA thermograms of the UG and CUG films under a nitrogen atmosphere

TABLE-3
THERMAL BEHAVIOUR OF THE UG AND CUG FILMS

Samples	T_{10} (℃)	T_{50} (℃)	T_i (℃)	T_f (℃)	Residue of 600 ℃ (wt %)
WPU	343	381	357	402	6.3
UG-20	262	374	249	407	11.2
UG-40	251	369	248	394	18.2
UG-60	220	367	246	395	25.2
UG-80	207	340	246	388	29.3
CMGG	137	289	247	290	27.4
CWPU	292	394	361	419	18.1
CUG-20	286	384	267	399	30.1
CUG-60	259	381	255	377	36.4
CUG-80	243	365	254	375	38.5
CCMGG	227	319	258	311	39.9

Surface properties and moisture absorption of the blended films: The contact angle of the UG and CUG films as a function of CMGG content was shown in Fig. 9. The CMGG film exhibited a relatively low contact angle of θ = 36° and the contact angle decreased rapidly after water droplet deposition. The water droplet was totally absorbed into the CMGG film in less than 1 min, which confirmed CMGG surface was hydrophilic and highly wettable. The pure WPU films exhibited a relatively high contact angle of θ = 69°. In the UG films, when WPU was blended with CMGG, the θ value of the films significantly decreased from 42 to 64°. Interestingly, the θ value of the CUG films was higher than that of the UG films. This
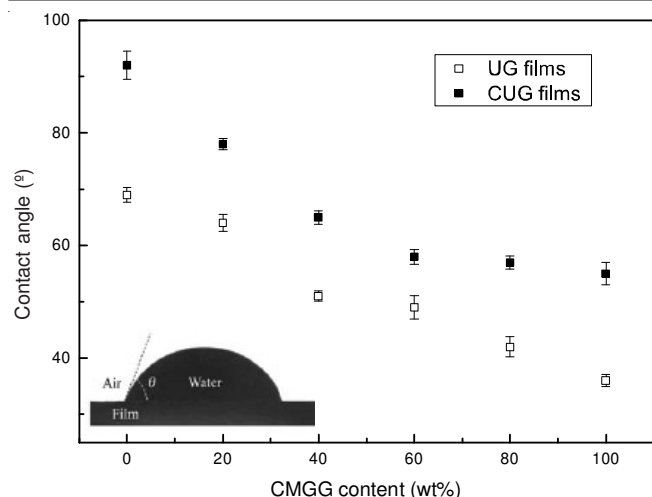
Fig. 9. Contact angles of the UG and CUG films as a function of CMGG content

indicated that the hydrophilic carboxylic group was chelated with Ca^{2+}, which made the CUG films a little hydrophobic than that of the UG films.

Moisture uptakes at equilibrium conditioned at 75 % RH for the UG and CUG films as a function of CMGG content was shown in Fig. 10. It is observed that CMGG absorbs 52 % moisture, which expressed nearly 0.52 g of moisture per gram of CMGG. The dashed line was the theoretical values of equilibrium moisture uptake, $WU_{(theory)}$, obtained from the additivity rule as the following equation:
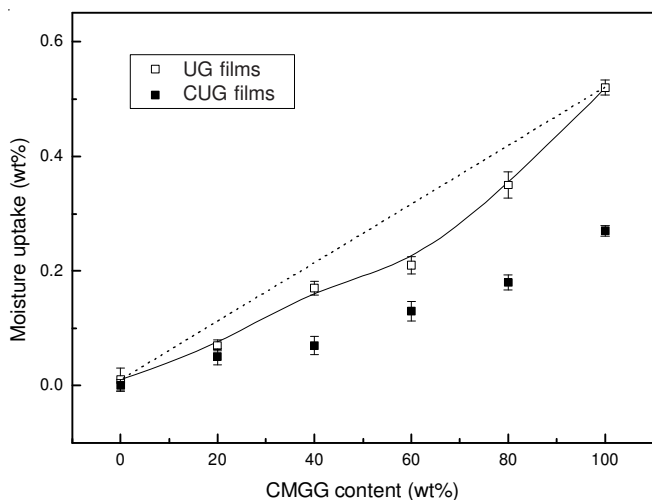
$$WU_{(theory)} = w_{GG}WU_{GG} + w_{PU}WU_{PU}$$

Fig. 10. Moisture uptakes at equilibrium conditioned at 75 % RH for the UG and CUG films as a function of CMGG content ("…", the dashed line was expressed to the theoretical moisture uptake of the UG films)

Where WU and w are, respectively, the equilibrium moisture uptake and mass fraction in the blends. Compared with theoretical values, a lower moisture uptake at equilibrium is observed for the UG films and only 17 % of moisture uptake for the film containing 40 wt % CMGG, indicating that some morphology differences of those hydrogen bonded blends with that of the physical blends. The moisture uptake of the blends increased non-linearly with increasing CMGG content. This behavior suggested occurrence of strong hydrogen bonding

interaction between WPU and CMGG. This interaction tends to stabilize and prevents the swelling of the CMGG matrix in high moisture environment, leading to a reduction of the moisture absorption. Meanwhile, the moisture uptake of the CUG films is little similar to that of the UG films. Interestingly, the moisture uptake of the CUG films was lower than that of the UG films and only 7 % of moisture uptake for the film containing 40 wt % CMGG. This phenomenon can be ascribed that the hydrophilic carboxylic group was chelated with Ca^{2+} in the CUG films. The Ca^{2+} crosslinking tends to stabilize and prevents the swelling of the CMGG matrix in high moisture environment, leading to a reduction of the moisture absorption.

Solvent-resistance of the blend films: The solvent-swelling tests are good methods to determine the solvent-resistance of blend films. The films in various solvents were swollen for 12 h and the results are summarized in Fig. 11. It is well known that most WPUs are linear thermoplastic polymers with very little gel content, which allows solubility in some organic solvents. When the CMGG content increased, there was a rapid decrease in the swelling degree of the UG films. Especially, when the CMGG content exceeded 60 wt %, the swelling degree remained at a very low value, which indicated CMGG played an important role in the enhancement of the solvent-resistance for the UG films. Fig. 11 also shows the solvent-swelling tests of the CUG films for 12 h. The solvent-resistance of the CUG films increased with an increase of CMGG content and the CUG films appeared higher chemical resistance than that of the UG films, which was attributed to its crosslinked structure.

Mechanical properties of the blend films: The dependency of the tensile strength (σ_b) and elongation at break (ε_b) on CMGG content for the UG and CUG blend films is shown in Fig. 12. The σ_b values for the UG films increased from 2.9 to 31.2 MPa with an increase of CMGG content from 20 to 80 wt % and the maximum value was observed at 80 wt% CMGG content. Interestingly, the CUG films all showed higher tensile strength than that of the UG films. The maximum value 56.5 MPa was also observed at 80 wt % CMGG content, indicating that the Ca^{2+} crosslinking structure from WPU and CMGG enhanced the mechanical strength of the blended films. WPU is a kind of typical flexible elastomer, which ε_b values of the blend was 1201.6%. With an increase of CMGG content, the ε_b values of the blend films decreased dramatically in the UG films. The elongation values of the CUG films were all lower than those of UG films, indicating that Ca^{2+} crosslinking had improved the toughness of the films through the formation of the Ca^{2+}-chelating structure. In the blended films, WPU film has poor tensile strength, which is hardly to be accepted in practical applications. However, the mechanical properties of the WPU films were improved greatly, owing to strong intermolecular hydrogen bonding between two polymers and the formation of Ca^{2+}-chelating structure in the blends.

Model describing the Ca^{2+} crosslinking structure of the blended films: In review of the results mentioned above, the crosslinked films possessed better miscibility and higher density, storage modulus, thermal stability, contact angle and tensile strength than the uncrosslinked films over the entire composition range. This is due to that the more uniform and dense architecture caused by Ca^{2+} crosslinking in the CUG films
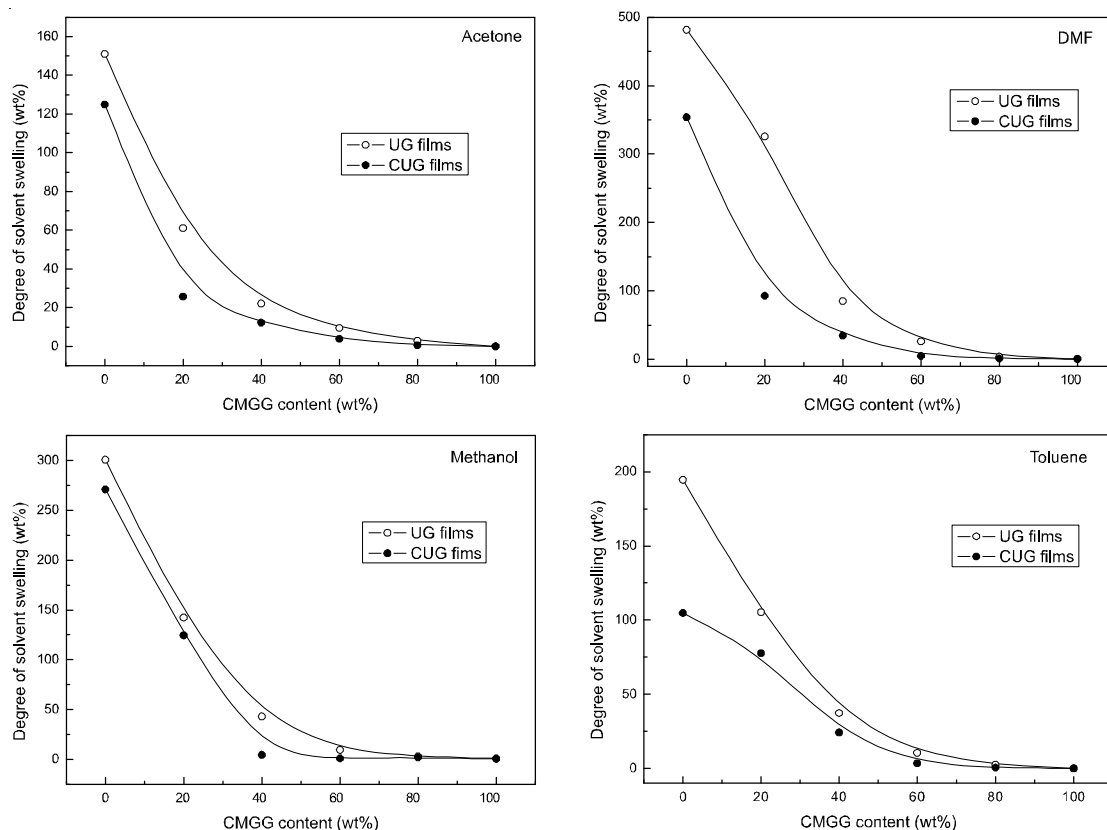
Fig. 11. Solvent-swelling degree of the UG and CUG films as a function of CMGG content
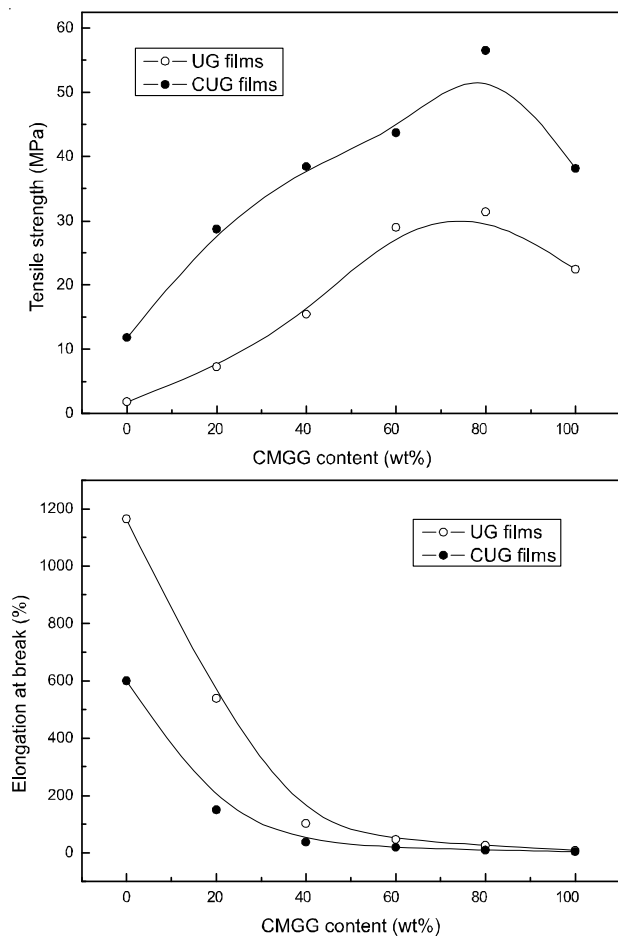

Fig. 12. Tensile strength (σ_b) and elongation at break (ε_b) of the UG and CUG films as a function of CMGG content

than that of the UG films. A model describing the crosslinking network formation by Ca^{2+} ion was proposed to illustrate the differences of their structures and properties as shown in Fig. 13. When CMGG content was relatively low, CMGG molecules penetrated into the WPU particles matrix and formed a dispersed phase. With an increase of CMGG content in the UG films, the CMGG phase domain size gradually grew up to achieve solid matrix. As CMGG content further increased, a small amount of WPU particles still existed, which dispersed into the CMGG continuous phase and formed the typical "island-sea" structure.

In addition, when the blend system was immersed into CaCl$_2$ aqueous ethanol solvents, the carboxylic groups containing CMGG or PU are coordinated with Ca^{2+}, resulting in the formation of chain-Ca^{2+}-chain interactions and forming interpenetrating polymer networks structure. The Ca^{2+}-chelating structure was helpful to improve relatively dense architecture of the blend films and compel the compatibility between WPU and CMGG. As also shown in Figs. 2 and 3, segregation morphology for the UG film formed in inner when CMGG content was relatively high. When Ca^{2+} was introduced into the blend system, uniform and densely packed architecture appeared in the CUG films.

Conclusion

Films from WPU and CMGG were prepared using the solution casting method and then crosslinked with calcium chloride. The results revealed that the blend film had higher thermal stability and tensile strength than that of the WPU film, suggesting good miscibility between WPU and CMGG. It was worth noting that the CUG films exhibited better miscibility
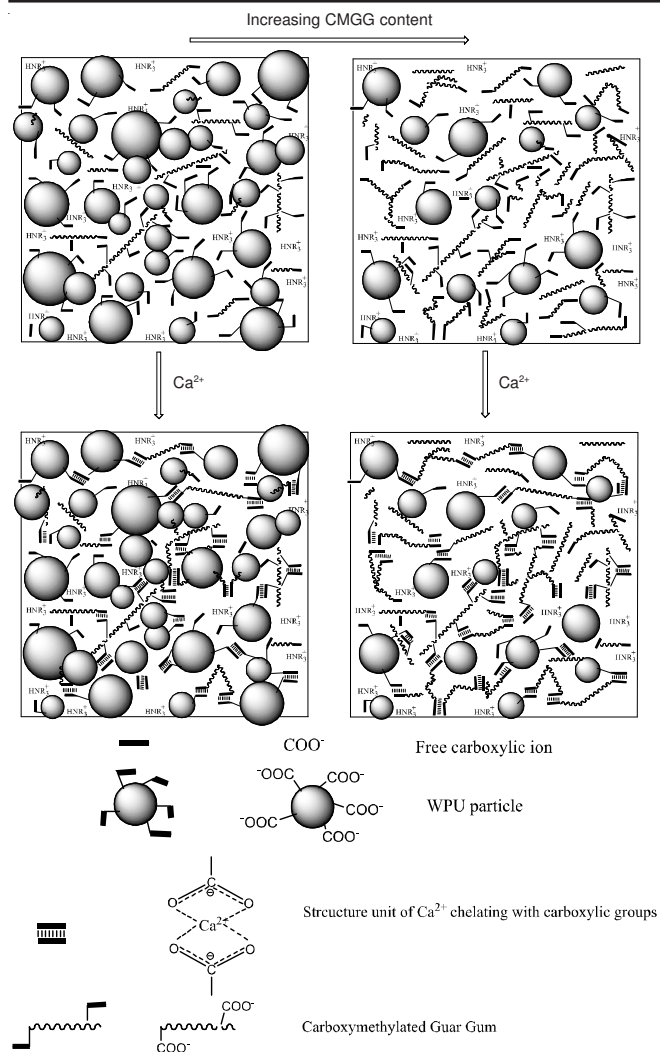
Increasing CMGG content

COO⁻   Free carboxylic ion

WPU particle

Strcuture unit of Ca²⁺ chelating with carboxylic groups

Carboxymethylated Guar Gum

Fig. 13. Schematic diagrams of the model describing the crosslinking network formation of the CUG films by Ca²⁺ ion

and higher density, storage modulus, thermal stability and tensile strength than that of the UG films over the entire composition range studied here. This difference can be attributed to the stronger entanglement and formation of a Ca²⁺ crosslinking structure between WPU and CMGG macromolecules in the CUG films. The structure, miscibility and properties of the crosslinked films depended significantly on Ca²⁺ crosslinking and the crosslinking structure can effectively improve the miscibility and properties of the blend films. A model describing the formation and structure of Ca²⁺ crosslinking was proposed here to illustrate the effect of the crosslinking on the WPU/CMGG blend films. Therefore, we provided a new method for preparing composite materials with excellent mechanical properties from natural polymers.

ACKNOWLEDGEMENTS

REFERENCES

1. S. Abouzahr and G.L. Wilkes, *J. Appl. Polym. Sci.*, **29**, 2695 (1984).
2. C. Alperin, P.W. Zandstra and K.A. Woodhouse, *Biomaterials*, **26**, 7377 (2005).
3. A.R. Kulkarni, K.S. Soppimath, T.M. Aminabhavi, A.M. Dave and M.H. Mehta, *J. Appl. Polym. Sci.*, **73**, 2437 (1999).
4. I. Arvanitoyannis, *J. Molec. Sci.-Rev. Macromol. Chem. Phys.*, **C39**, 205 (1999).
5. I. Arvanitoyannis, I. Kolokuris, A. Nakayama and S.- Aiba, *Carbohydr. Polym.*, **34**, 291 (1998).
6. E. Brinkman and P. Vandevoorde, *Progr. Org. Coat.*, **34**, 21 (1998).
7. G.L. Brode, E.D. Goddard, W.C. Harris and G.A. Salensky, In eds.: C.G. Gebelein, T.C. Cheng and V.C. Yang, Plenum, Cationic Polysaccharides for Cosmetics and Therapeutics, In Cosmetic and Pharmaceutical Applications of Polymers, New York, pp. 117-128 (1991).
8. X. Cao, L. Zhang, J. Huang, G. Yang and Y. Wang, *J. Appl. Polym. Sci.*, **90**, 3325 (2003).
9. R. Chandra and R. Rustgi, *Biodegrad. Polym. Progr. Polym. Sci.*, **23**, 1273 (1998).
10. Y. Cheng, K.M. Brown and R.K. Prud'homme, *Biomacromolecules*, **3**, 456 (2002).
11. D. Demirgoz, C. Elvira, J.F. Mano, A.M. Cunha, E. Piskin and R.L. Reis, *Polym. Degrad. Stab.*, **70**, 161 (2000).
12. D. Dieterich, *Progr. Org. Coat.*, **9**, 281 (1981).
13. V. Duecoffre, W. Diener, C. Flosbach and W. Schubert, *Progr. Org. Coat.*, **34**, 200 (1998).
14. J.E. Fox, In ed.: A. Imeson, Seed Gums, In Thickening and gelling agents for food, Blackie Academic Professional, New York, edn. 2, pp. 262 (1997).
15. G. Freddi, M. Tsukada and S. Beretta, *J. Appl. Polym. Sci.*, **71**, 1563 (1999).
16. I. Gliko-Kabir, B. Yagen, M. Baluom and A. Rubinstein, *J. Control. Rel.*, **63**, 129 (2000).
17. D.J. Hourston and F.U. Schafer, *Polymer*, **37**, 3521 (1996).
18. B.K. Kim, T.K. Kim and H.M. Jeong, *J. Appl. Polym. Sci.*, **53**, 371 (1994).
19. B.K. Kim, J.W. Seo and H.M. Jeong, *Eur. Polym. J.*, **39**, 85 (2003).
20. S.C. Kim, D. Klempner, H.L. Frisch, W. Radigan and H.L. Frisch, *Macromolecules*, **9**, 258 (1976).
21. S.R. Kim, S.H. Yuk and M.S. Jhon, *Eur. Polym. J.*, **33**, 1009 (1997).
22. S. Kobayashi, S. Tsujihata, N. Hibi and Y. Tsukamoto, *Food Hydrocoll.*, **16**, 289 (2002).
23. R. Lapasin and S. Pricl, Applications of Guar Gum Derivatives, In Rheology of Industrial Polysaccharides: Theory and Applications, Blackie Academic and Professional, London, pp. 145-149 (1995).
24. D.S. Lee and T.S. Park, *J. Appl. Polym. Sci.*, **43**, 481 (1991).
25. Y.-H. Lin, S.-C.J. Hwang, W.-C. Shih and K.-C. Chen, *J. Appl. Polym. Sci.*, **99**, 738 (2006).
26. Y. Lu, L. Tighzert, P. Dole and D. Erre, *Polymer*, **46**, 9863 (2005).
27. M. Mathew, K.N. Ninan and S. Thomas, *Polymer*, **39**, 6235 (1998).
28. K.-L. Noble, *Progr. Org. Coat.*, **32**, 131 (1997).
29. C.S. Paik Sung, T.W. Smith and N.H. Sung, *Macromolecules*, **13**, 117 (1980).
30. D.P. Queiroz, M.N. de Pinho and C. Dias, *Macromolecules*, **36**, 4195 (2003).
31. K.S. Soppirnath and T.M. Aminabhavi, *Eur. J. Pharm. Biopharm.*, **53**, 87 (2002).
32. A. Tayal, V.B. Pai and S.A. Khan, *Macromolecules*, **32**, 5567 (1999).
33. L.S. Teo, C.Y. Chen and J.F. Kuo, *Macromolecules*, **30**, 1793 (1997).
34. R.N. Tharanathan, *Trends Food Sci. Technol.*, **14**, 71 (2003).
35. N. Wang and L. Zhang, *Polym. Int.*, **54**, 233 (2005).
36. T.C. Wen, M.S. Wu and C.-H. Yang, *Macromolecules*, **32**, 2712 (1999).
37. P.J. Whitcomb, J. Gutowski and W.W. Howland, *J. Appl. Polym. Sci.*, **25**, 2815 (1980).
38. R.H.W. Wientjes, M.H.G. Duits, R.J.J. Jongschaap and J. Mellema, *Macromolecules*, **33**, 9594 (2000).
39. N. Wang, L. Zhang, Y. Lu and Y. Du, *J. Appl. Polym. Sci.*, **91**, 332 (2004).
40. X. Xu, L. Wang, H. Toghiani and C.U. Pittman, *J. Appl. Polym. Sci.*, **78**, 1402 (2000).
41. G. Yang, Q. Huang, L. Zhang, J. Zhou and S. Gao, *J. Appl. Polym. Sci.*, **92**, 77 (2004).